

# Absorption Analysis of Electron Cyclotron Waves in the Magnetospheric Plasma Device RT-1<sup>\*)</sup>

Takahiro MORI<sup>1)</sup>, Masaki NISHIURA<sup>1,2)</sup>, Naoki KENMOCHI<sup>2)</sup>, Kenji Ueda<sup>1)</sup>, Takuya Nakazawa<sup>1)</sup> and Zensho Yoshida<sup>2)</sup>

<sup>1)</sup>Graduate School of Frontier Sciences, The University of Tokyo, Kashiwa, Chiba 277-8561, Japan

<sup>2)</sup>National Institute for Fusion Science, Toki 509-5292, Japan

(Received 10 January 2022 / Accepted 1 June 2022)

The absorption efficiency of electron cyclotron heating is investigated theoretically and experimentally to understand the wave heating mechanisms under the overdense state and the density limit. The features of self-organizing mechanisms have been observed in the dipole confinement system [M. Nishiura *et al.*, Nucl. Fusion **55**, 053019 (2015)]. The modulated 2.45 GHz electromagnetic (EM) wave is applied to the RT-1 plasmas to evaluate the EM wave's absorption efficiency from the diamagnetic signals' response. The absorption efficiency maintains a constant 100% beyond the O-mode's cutoff density. However, it decreases rapidly near the  $1.6 \times 10^{17} \text{ m}^{-3}$  line-averaged density, which is twice higher than the 2.45 GHz O-mode cutoff. At less than  $0.6 \times 10^{17} \text{ m}^{-3}$ , the absorption efficiency simulated by a ray-tracing code in a two-dimensional model explains the experimental absorption efficiency. However, it deviates from the experimental value near the cutoff density and is more significant at the density limit. We discuss the difference between the experimental and numerical results.

© 2022 The Japan Society of Plasma Science and Nuclear Fusion Research

Keywords: magnetospheric plasma, electron cyclotron heating, electron cyclotron wave, overdense plasma, electromagnetic wave propagation

DOI: 10.1585/pfr.17.2405090

## 1. Introduction

The dipole field, a basic natural structure for plasma confinement, is appropriate for extracting principal and universal physics. The Ring Trap 1 (RT-1) is inspired by the Jovian magnetosphere. The self-organized plasma formation in the Jovian magnetosphere motivates us to examine a plasma confinement system. The RT-1 enables us to study magnetospheric plasma physics and advanced fusion. The RT-1 device demonstrated the plasma confinement in a dipole field by a levitated superconducting ring magnet [1].

The plasmas are produced by electron cyclotron heating (ECH) with 2.45 GHz and/or 8.2 GHz electromagnetic (EM) waves. The produced plasmas form a peaked density profile, a self-organized structure observed in naturally-formed planetary magnetospheres. It is observed that the line-averaged electron density is limited below the 8.2 GHz EM wave's cutoff density. However, the 2.45 GHz EC wave usually overcomes the 2.45 GHz cutoff density experimentally, although the same interferometer was used. Understanding the propagation and absorption of EM waves is essential to distill the underlying physics from the apparent density limits in 8.2 and 2.45 GHz EC heating schemes. To clarify the relationship between the wave absorption and heat transport in the magnetospheric plasma,

we studied the propagation and absorption with full-wave simulation [2]. However, it is still unclear whether the phenomena are caused by the dipole confinement system's inherent magnetic structure and inhomogeneous medium.

Our goal is to comprehend the plasma production in an inhomogeneous region of a dipole plasma confinement system under the self-organized plasmas, and extend the regime of the operation region (overdense heating and thermal particle transport). This study investigates the propagation and absorption of EM waves experimentally and numerically.

## 2. Magnetospheric Plasmas in the RT-1

Figure 1 shows the EC heating system and main diagnostics of the RT-1 device. The vacuum vessel's interior is evacuated to  $10^{-6}$  Pa. The working gas (hydrogen or helium) is filled in the vacuum vessel in the range of more than  $10^{-4}$  Pa, and the ECH produces and sustains plasmas.

For the ECH, an EM wave from an 8.2 GHz klystron (Toshiba, nominal power 100 kW) is launched from the upper ports through the transmission lines L#1 and L#2 obliquely toward the fundamental electron cyclotron resonance (ECR) layer, which lies across the levitated magnet. The EM wave propagates via the plasma edge region to access the absorption layer. In the RT-1 experiment, the line integral density was measured using the interferometer 1

author's e-mail: mori.takahiro@nifs.ac.jp

<sup>\*)</sup> This article is based on the presentation at the 30th International Toki Conference on Plasma and Fusion Research (ITC30).

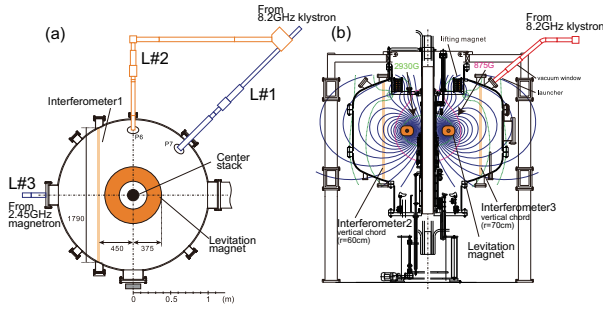


Fig. 1 Overview of the RT-1 device. (a) is the equatorial plane and (b) is a poloidal cross-section. The transmission lines L#1 and L#2 are for the 8.2 GHz EC heating, and L#3 is for the 2.45 GHz. The line integral density was measured by the interferometer 1-3 (IF 1-3). IF 1 measures the line integral density horizontally, and IF 2 and 3 measure it vertically. The chord length of the IF 1 was 1.6 m, estimated from two points on the chord where the last closed flux surface crosses at the midplane.

(IF 1). The chord length of the IF 1 was 1.6 m, estimated from two points on the chord where the last closed flux surface crosses at the midplane. The line integral density divided by the chord length yields the line-averaged density. The injection power was changed from 0 to 40 kW to characterize the density limit for the 8.2 GHz ECH. The helium filling gas pressure ranged from 3 to 28 mPa. The density limit appears at the electron density of  $8.0 \times 10^{17} \text{ m}^{-3}$  for the 8.2 GHz ECH [3]. According to the results of the density reconstruction with interferometry, the core density reached the so-called overdense state.

Meanwhile, an EM wave from a 2.45 GHz magnetron (with nominal power of 20 kW) is introduced into the vacuum vessel from the equatorial port through the transmission line L#3. The EM wave propagates perpendicular to the magnetic fields for the fundamental O-mode heating. The EM wave experiences a peaked density region to reach the ECR layer. The fundamental ECR layer lies across the plasma in the confinement region. We investigated the experimental density limit for the 2.45 GHz ECH and the injection power was changed from 0 to 18 kW. The filling gas pressure of helium ranged from 1.65 to 18.9 mPa. The density limit appeared at  $\bar{n}_e = 1.6 \times 10^{17} \text{ m}^{-3}$  [2].

### 3. Evaluation of the ECH Absorption at the RT-1

The absorption power of the EM waves can be evaluated experimentally from the time variation of the plasma storage energy [4]. The time variation of stored energy when the ECH turns off can be expressed as follows:

$$\frac{dW_{p0}}{dt} = -\frac{1}{\tau_{E0}} W_{p0} - P_{rad0}. \quad (1)$$

When the ECH turns on, the equation becomes the following:

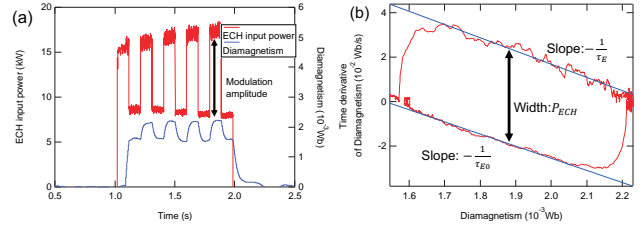


Fig. 2 (a) ECH output modulation and diamagnetic signal response. (b) Diamagnetic signal response and its time derivative at one period of ECH turn on and off.

$$\frac{dW_{p1}}{dt} = -\frac{1}{\tau_{E1}} W_{p1} - P_{rad1} + P_{ECH}, \quad (2)$$

where  $W_p$ ,  $\tau_E$ ,  $P_{rad}$ , and  $P_{ECH}$  are the stored energy, confinement time, plasma radiation power, and ECH power, respectively. The subscripts 0 and 1 indicate the values when the ECH is off and on. The plasma condition is unchanged because the modulation time is smaller than the confinement time, and we assumed  $\tau_{E0} = \tau_{E1}$ ,  $P_{rad0} = P_{rad1}$ , and  $W_{p0} = W_{p1}$ . Under these assumptions, the plasma absorption efficiency is presented as follows:

$$P_{ECH} = \left( \frac{dW_{p0}}{dt} - \frac{dW_{p1}}{dt} \right). \quad (3)$$

Using eq. (3), the ECH absorption power can be evaluated from the difference in the time derivative of the plasma stored energy when the ECH is turned on and off. The relationship between the plasma diamagnetic signal and the local electron beta value was revealed in a previous study [3]. We calculated the relationship between the plasma diamagnetic signal and the stored energy as  $1 \text{ mWb} = 150 \text{ J}$  from this result and the plasma volume. In this paper, the absorbed power is quantified using the above equation.

When the ECH input is turned off, the plasma disappears completely, and the state of the plasma changes significantly. Therefore, in this study, instead of repeating the on-off of the ECH, the incident power of the ECH is increased or decreased in a certain period, and the response of the plasma's diamagnetic signal is not significantly changed. Figure 2(a) shows the time evolution of the input power and the diamagnetic signal when the ECH is modulated at a 5 Hz frequency (hereafter, this operation is called ECH modulation). At the ECH modulation, the maximum and minimum input powers are  $P_{max}$  and  $P_{min}$ , respectively, the modulation amplitude is  $P_{max} - P_{min}$ , and the modulation ratio is  $(P_{max} - P_{min})/P_{max}$ . The filling gas is helium, and the gas pressure is set to 2.36 mPa. Furthermore, the diamagnetic signal also responds to the ECH modulation and changes in the same period as the ECH in about 2.2 mWb to 1.6 mWb range. The density changes only a few percent during the modulation, which is smaller than the amount of change in the diamagnetic signals.

However, inductance is a factor that slows down the time response of the diamagnetic signal measurement.

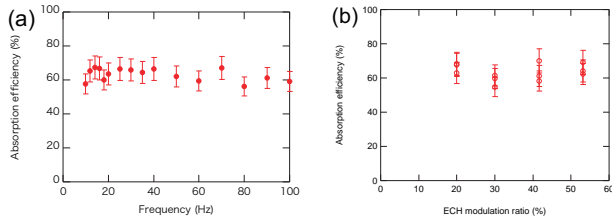


Fig. 3 ECH efficiency's dependence on the modulation frequency and ratio. The helium gas pressure is 1.77 mPa ( $\bar{n}_e \approx 1.4 \times 10^{17} \text{ m}^{-3}$ ) and the maximum ECH input power is 17 kW. (a) ECH efficiency's dependence on the modulation frequency (modulation ratio is 40%). (b) ECH efficiency's dependence on the modulation ratio (modulation frequency is 5 Hz).

Here, we consider whether the measurement's time response is sufficiently fast even when there is a sudden change, such as immediately after the start of the ECH. Figure 2 (b) shows the relationship between the plasma's time response and its time derivative from the last 1.8 s to 2.0 s measured by the diamagnetic signal measurement in the ECH modulation experiment. The slope  $(\frac{dW_p}{dt})/(W_p)$  matches  $-1/\tau_E$  and the amount of absorption is evaluated from the difference between the two line segments that show  $\tau_E$ . The absorption efficiency is obtained by dividing the absorption amount by the modulation amplitude.

We investigated the frequency and modulation ratio dependence when evaluating the absorption efficiency of the ECH modulation. Figure 3 shows that the dependence of the absorption efficiency does not appear clearly in the frequency range (10 - 100 Hz) and modulation ratio (20% - 60%). Therefore, the absorption efficiency was evaluated with a frequency of 10 Hz and an amplitude of 10% - 50%.

Consequently, we investigated the plasma's power absorption efficiency with respect to the electron density when the modulation frequency is 10 Hz, the ECH power modulation amplitude is 4 kW, the maximum ECH input power is changed in the range of 4 - 17 kW, and the He gas pressure was changed in the range of 1.77 - 11.8 mPa. The result is shown in Fig. 4. The experimental result shows that the plasma's power absorption efficiency at the low-density state is about 100%, which is maintained at 100% even in the region where the cutoff density ( $n_e \approx 0.8 \times 10^{17} \text{ m}^{-3}$ ) is exceeded. However, when the line-averaged electron density exceeds the cutoff density, the plasma's power absorption efficiency decreases gradually. At the density limit region at RT-1,  $\bar{n}_e = 1.6 \times 10^{17} \text{ m}^{-3}$ , the plasma's power absorption efficiency drops rapidly to less than 20%. We developed a two-dimensional (2D) ray-tracing simulation to clarify the experimental result.

#### 4. Ray-tracing Simulation in the RT-1 Plasma

We simulated the propagation of 2.45 GHz EM waves in the plasmas using ray-tracing simulation [5]. The prop-

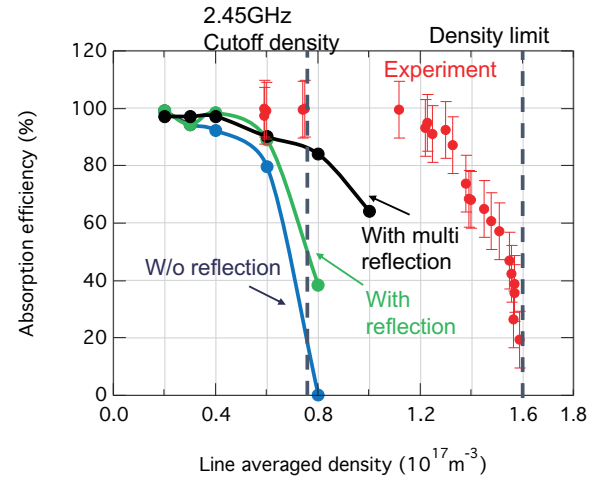


Fig. 4 The dependence of the absorption efficiency on the electron density. Closed red circle is the experimental absorption efficiency and blue, green, and black curves indicate the ray-tracing ones without, with, and multi-reflection on the vacuum vessel.

agation of the EM waves in slightly inhomogeneous plasmas can be sufficiently described within the WKB approximation, also called the geometrical optics approach [6]. The ray trajectory in the ray-tracing simulation can be defined as a solution of the characteristic equations given as follows:

$$\frac{d\mathbf{r}}{dt} = \frac{\partial D}{\partial \mathbf{k}} \left| \frac{\partial D}{\partial \omega} \right|, \quad (4)$$

$$\frac{d\mathbf{k}}{dt} = \frac{\partial D}{\partial \mathbf{r}} \left| \frac{\partial D}{\partial \omega} \right|. \quad (5)$$

Here,  $\mathbf{r}$  and  $\mathbf{k}$  are the radius vector and wave number vector, respectively.  $D$  is the dispersion tensor [7]. The propagating EM wave in the plasmas could be obtained by solving the radius and wave number at each position along the wave's trajectory.

In the ray-trace simulation, we used the same magnetic field profile and electron density employed in a previous study [2]. The peak density for the line-averaged density of  $\bar{n}_e = 1.6 \times 10^{17} \text{ m}^{-3}$  is  $n_0 = 3.5 \times 10^{17} \text{ m}^{-3}$ . In the following simulation,  $n_0$  is changed while maintaining other profile parameters.

Figure 5 is the result of the ray-tracing calculation where the center density is  $n_0 = 6.0 \times 10^{16} \text{ m}^{-3}$  (near the cutoff density) and O-mode injection of the ECH. The incident position is  $r = 0.99 \text{ m}$ ,  $-0.2 \text{ m} < z < 0.2 \text{ m}$ , and the rays are uniformly distributed. Even at a density far lower than the current density limit, a part of the rays can reach the ECR layer, but some parts cannot. The rays are significantly bent in the plasma when the central density increases further; thus, they cannot reach the resonance layer. Considering the reflection of the rays at the vacuum vessel [shown in Fig. 5 (b)] increases the possibility of the rays reaching the resonance layer and explaining the experi-

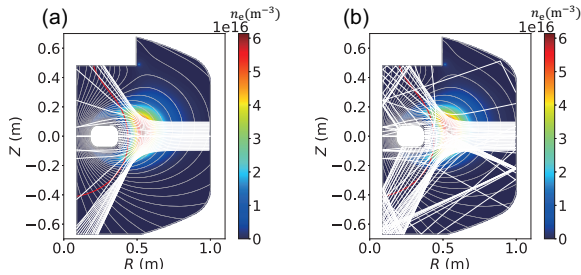


Fig. 5 Ray-tracing simulation result at  $n_0 = 6.0 \times 10^{16} \text{ m}^{-3}$ . The red line shows the 2.45 GHz fundamental resonance layer and the white lines shows the ray's trajectory. (a) is the result without the reflection at vacuum vessel and (b) is the result with the reflection at the vacuum vessel.

mental results. In this study, we calculated the three ray-trace situations. One is without reflection, another is with double reflections, and the other is with multiple reflections, in which the maximum reflection number is a hundred, and each ray loses 3% energy at the wall reflection.

We applied the weakly relativistic absorption model for O- and X-modes derived by Bornatici [8]. This model has been used in the LHD-GAUSS [9]. The LHD-GAUSS-U code [10] has been upgraded to realize a more precise solution even though an oblique injection to magnetic fields. We will implement this model to evaluate wave absorption. The electron temperature is assumed to be uniform at 100 eV, which is the maximum bulk electron temperature. Figure 4 shows the result.

If the reflection is not considered, the absorption efficiency drops sharply when the 2.45 GHz cutoff density is exceeded and becomes 0 thereafter. However, the deterioration of the absorption efficiency is improved when the vacuum vessel reflection is assumed, although there is no explanation for the absorption efficiency being maintained at 100% up to the region exceeding the cutoff density, as in the experimental results. This calculation result shows that it is enough for the 2D simulation to explain the experimental result under the cutoff density state. Moreover, to explain the experimental result, it is necessary to consider the effect of ray wraparound by three-dimensional (3D) calculation and multiple reflections on the vacuum vessel at the RT-1.

## 5. Discussion

The modulated 2.45 GHz EM wave is applied to the RT-1 plasmas to evaluate the EM wave's absorption efficiency. The response of the diamagnetic signal is analyzed to obtain the absorption power and energy confinement time. While the line-averaged density increases, the absorption efficiency remains constant at 100% beyond the 2.45 GHz cutoff density to  $\bar{n}_e = 0.8 \times 10^{17} \text{ m}^{-3}$ . The absorption efficiency gradually decreases to zero when the line-averaged density increases further. The density's upper limit appears at  $\bar{n}_e = 1.6 \times 10^{17} \text{ m}^{-3}$ , which is twice

higher than the 2.45 GHz O-mode cutoff.

A ray-tracing code in a 2D model simulates the propagation of the EM waves with a cold plasma approximation and the absorption with a hot plasma one in the RT-1 plasmas. We cannot explain the experimental absorption efficiency in the overdense state so far by the simulation result even if we consider the multireflection of the rays at the vacuum vessel. The discrepancy might be caused by the 3D geometrical effect, accessible to the ECR layer from the high field side, and mode scramble by the multireflection. Consequently, we extend the ray-tracing simulation code from the 2D model to the 3D model and will discuss the mode scramble effect in the 3D simulation. This simulation assumed a uniform electron temperature in the RT-1 plasmas. It is necessary to measure the electron temperature profile, including the temperature dependence on the electron density, and apply it to the calculation. The high-energy (>10 keV) electrons, which form the toroidal 'belt' structure in the outer region, are measured using X-ray detectors [11]. The high-energy electron density is about two orders of magnitude lower than the bulk electron density; however, the high-energy electrons' absorption rate is large. Therefore, we consider calculating the high-energy electrons' effect on the wave absorption using a two-component temperature model in the future.

The present simulation cannot explain the experimental overdense states and density limits in view of the power absorption. Another possible absorption under the overdense plasmas might be a mode conversion to EBW [12]. In a dipole plasma confinement, the created density profiles at the peak exceed the cutoff densities at both frequencies. We clarify the ECH effect and divide the self-organization effect with uphill diffusion [1]. Further study is needed to understand the density limit and the heat transport in the magnetospheric plasmas of the RT-1.

## 6. Conclusion

The EC wave's absorption power efficiency was evaluated experimentally by ECH power modulation in RT-1 plasma experiments. The power of the EC wave absorbs even in the overdense state, and it decreases drastically near the density limit. We have developed a ray-tracing calculation to explain the experimental absorption efficiency in the overdense state. The ray-tracing calculations explain the experimental absorption efficiency well below the cutoff density. However, it cannot explain the experimental one adequately in the overdense state, even though it contains the EC waves' multireflection on the wall surface. We will extend the ray-tracing code for 3D calculation and a mode conversion effect.

## Acknowledgments

The authors would like to thank Dr H. Saitoh of the University of Tokyo for the discussion. This work was supported by the JSPS KAKENHI (Grant Numbers 17H01177

and 19KK0073), NIFS collaboration research program (NIFS19KBAR026), and JST SPRING (Grant Number JP-MJSP2108).

- [1] Z. Yoshida *et al.*, *Phys. Plasmas* **17**, 112507 (2010).
- [2] T. Mori *et al.*, *Plasma Fusion Res.* **55**, 3401134 (2019).
- [3] M. Nishiura *et al.*, *Nucl. Fusion* **55**, 053019 (2015).
- [4] R. Makino *et al.*, *JPS Conf. Proc.* **1**, 015034 (2014).
- [5] N.B. Marushchenko *et al.*, *Comput. Phys. Commun.* **185**, 165 (2014).
- [6] G. Bekefi, *Radiative Processes in Plasmas* (John Wiley & Sons, New York, 1966).
- [7] T.H. Stix, *Waves in Plasmas* (AIP press, 1992).
- [8] M. Bornatici *et al.*, *Nucl. Fusion* **23**, 1153 (1983).
- [9] S. Kubo *et al.*, *AIP Conf. Proc.* **669**, 187 (2003).
- [10] R. Yanai *et al.*, *Plasma Fusion Res.* **16**, 2402084 (2021).
- [11] M. Nishiura *et al.*, *Nucl. Fusion* **59**, 096005 (2019).
- [12] K. Uchijima *et al.*, *Plasma Fusion Res.* **6**, 2401122 (2011).